ISSN : 0974 - 7486 Volume 11 Issue 5

Materials Science

An Indian Journal

Full Paper

MSAIJ, 11(5), 2014 [195-200]

Iron pyrite thin films synthesized by spray pyrolysis technique

Saad Farhan Oboudi[1], Khudheir A.Mishjil[2], Nadir Fadhil Habubi[2]*, Sami Salmann Chiad[2]

[1]Baghdad University, College of Science, Physics Department, Baghdad, (IRAQ)

[2]Al_Mustansiriyah University, College of Education, Physics Department, Baghdad, (IRAQ)

E-mail: nadirf61@gmail.com

ABSTRACT

In this investigation, FeS_2 thin films were synthesized by spray pyrolysis technique on glass substrates. The films were annealed at 400 ºC and 450ºC in air for a period of 1 hour. The optical characterizations of the as deposited and annealed films were carried out using UV–VIS transmittance spectroscopy in the wavelength range 400–900 nm. The results show that in the visible region the transmittance of the films decreases as the annealing temperature increases to 450ºC. The reverse is the case with the reflectance as it was observed to be increased in the same region. The result also shows that the absorption coefficient, extinction coefficient, real and imaginary parts of dielectric constant are tending to increase with the increasing of annealing temperature. Further analysis shows that the films have high optical conductivity about 4.06-6.20 x $10^{14}S^{-1}$. The refractive index was found to be 4.38-5.14. The foregoing desirable properties make the FeS_2 to be a promising material for the fabrication of solar cells and optoelectronic devices.

KEYWORDS

Iron pyrite FeS_2;
Optical constants;
Spray pyrolysis technique.

INTRODUCTION

Iron pyrite FeS_2 has been widely investigated due to its potential photovoltaic and photoeletrochemical applications as a result of its proper band gap ($E_g \approx$ 0.95eV) and large absorption coefficient ($\alpha > 10^5 cm^{-1}$ for $\lambda < 103nm$)[1,2]. In addition, iron pyrite which consists of nontoxic and widely available elements, is a suitable semiconductor material for the environment. Therefore, it is attracting more attention because of its promising potentials for applications as optoelectronic and photovoltaic material[3-9].

Formation of a particular phase depends on the nature of the starting material, its composition, deposition method, and annealing temperatures. Many techniques were used to produce pyrite films such as sulfurization of electrodeposited[10,11], metalorganic chemical vapour deposition[12], ion beam magnetron sputtering[13], spray pyrolysis[14], electrodeposition[15,16], MOCVD[17], solvothermal synthesis method[18], magnetron sputtering[19] and Plasma-assisted sulfurization[20]. Each one of these methods has its own benefits which can be used to obtain films with specific characterizations.

Many researches have been devoted to study the fabrication and characterization of FeS_2 thin films. In a review of literatures, it can be seen that the effect of annealing parameters on the film characteristics should be studied more sufficiently. In this study, the optical characteristics of FeS_2 films deposited by spray py-

Full Paper

rolysis technique on glass substrates are reported. The optical constants of the films were examined and the effect of annealing temperature upon the optical properties of the films was investigated.

EXPERIMENTAL DETAILS

Iron pyrite FeS_2 thin films were deposited by the spray pyrolysis technique[21], using iron chloride $FeCl_2$ (purity: 99.99%) from Sigma-Aldrich UK and thiourea $CS(NH_2)_2$ (purity: 99.98%) from Merck Germany. The molarity of the prepared solution is 0.1 M. The $FeCl_2$ was dissolved in a mixture of methanol and redistilled water in the ratio of 1:1, while the thiourea was dissolved in deionized water. To enhance the solubility of $FeCl_2$, a few drops of HCl were also added. The prepared solutions of iron chloride and thiourea were appropriately mixed to obtain an Fe:S proportion of 1:2. The solutions obtained were pulverized on glass substrates with compressed air that maintained at a pressure of $10^5\,Nm^{-2}$ at a flow rate of 5 ml/min and deposition time 5 sec followed by 2 minutes wait to avoid excessive cooling. The substrate temperature was maintained at 400 °C. The distance from the spray nozzle to the heater was kept at approximately at 29 cm. Under these deposit conditions, good films are obtained. They are uniform and very adherent to the substrates.

The samples were weighed before and after spraying to determine the mass of the films[22]. Knowing the dimensions of the substrates used, the thicknesses can be determined using the following equation[23]:

$$d = \frac{\Delta m}{\rho_m\, lL} \qquad (1)$$

Where Δm is the difference between the mass after and before spraying, ρ_m is the density, l the width and L the length. Where Δm is the difference between the mass after and before spraying, ρ is the density, l the width and L the length. Optical transmittance and absorbance were recorded in the wavelength range (300-900 nm) using UV-VIS spectrophotometer (Shimadzu Company Japan). The effect of annealing temperatures on the optical properties was investigated.

RESULTS AND DISCUSSIONS

The spectral dependence of transmittance of the as deposited FeS_2 films and the films after annealing to 400 °C and 450 °C are shown in Figure 1. The results indicate that T increases with the increasing of the incident photons wavelength λ, and decreases with the increasing of annealing temperature. Also the figure announces that the percentage of transmission of the as deposited film is approximately 45% in the visible region, decreased to 25% and 20% by increasing the annealing temperature to 400 °C and 450 °C respectively. This could be attributed to the effect of point detects and film discontinuities from sulfuration at higher temperature. More vacancies should be created in the films annealed at 450°C because a lower energy of vacancy formation was calculated at the temperature. These point defects forming donor or accepter states in forbidden zones cause the reduction of band gap width[24]. Moreover, more film discontinuities or inhomogeneities, such as pinholes, peelings and irregular film morphology can be formed at 450°C. They tend to increase the transparency or decrease the film absorbency. As a result, it is possible to make the optical absorption edge move to low photon energies. This is in close agreement with the reports of Kassim et al[25] and Meng et al[26].

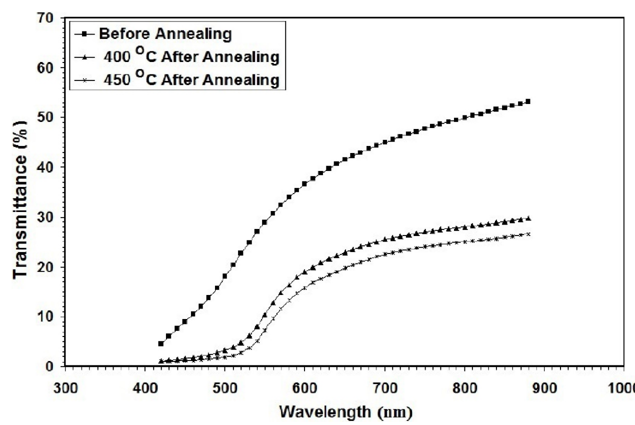

Figure 1 : Transmittance versus wavelength for as deposited and annealed FeS_2 thin films

Figure 2 shows that in the visible region, the reflectance average value of the as deposited films was about 0.38%, while the reflectance for the films after annealed to 400 °C and 450°C increased with the increasing of wavelength and have the average value of 0.45%. It can be seen that the reflectance in the visible region is limited only by the surface reflectance.

The optical properties of FeS_2 films by means of

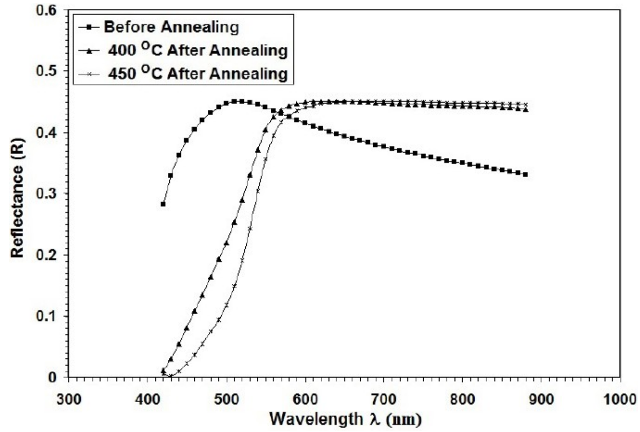

Figure 2 : Reflectance versus wavelength for as deposited and annealed FeS_2 thin films

optical absorption in the visible region of (400–900) nm have been investigated. The absorption coefficient (α) could be calculated using the following relation[27]:

$$\alpha = \frac{2.303A}{t} \quad (2)$$

Where (A) is the absorption and (t) is the film thickness. Figure 3 show the dependence of the absorption coefficient (α) of the as deposited and annealed FeS_2 films. It can be seen that with increasing annealing temperature the absorption edge shifts to a higher wavelength direction in the visible region. This result proves that the films are sensitive to visible light. The blue shift in the absorption band edge has been claimed as a consequence of exciton confinement with decrease particle size (the so-called quantum-size effect) in FeS_2 films. Also, it might be due to the change of the energy gap of the disorder crystal in the films.

The refractive index of the films is an important parameter for the optoelectronic device design. In order

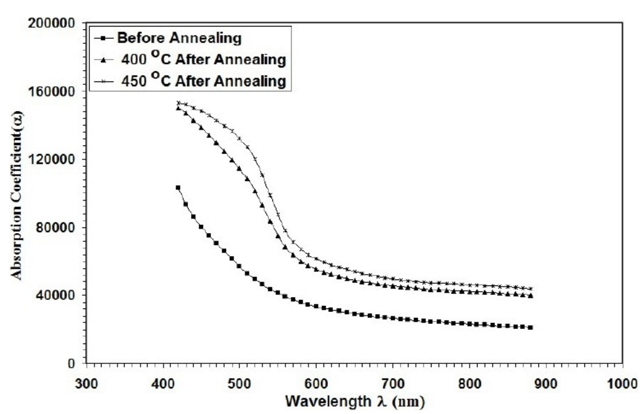

Figure 3 : Absorption coefficient versus wavelength for FeS_2 thin films

to calculate the optical constant refractive index (n) and the extinction coefficient (k) of the films at different wavelengths, we can use the following relations[28,29]:

$$n = [1 + R/1 - R] + [4R / (1-R)^2 - k^2]^{1/2} \quad (3)$$

$$k = \alpha\lambda/4\pi \quad (4)$$

Where (α) is the absorption coefficient and λ is the wavelength. The refractive index of the films was calculated by using Eq. (2) and the variation of refractive index with wavelength for the films is shown in Figure 4. After annealing to 400 ºC and 450ºC both films showed similar behavior in refractive index spectra which is a gradually increases with increasing wavelength. This increase may be attributed to the higher packing density and change in crystalline structure. Many researchers have reported that annealing treatment caused the refractive index to increase due to the enhancement of crystallization. Refractive index values of the samples have varied between (4.9-5.0) at long wavelengths.

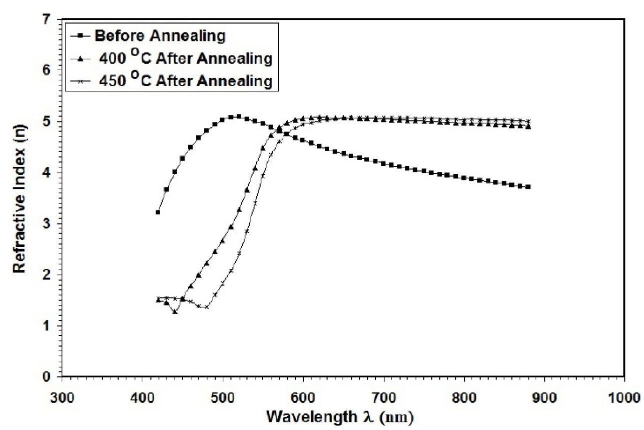

Figure 4 : Refractive index versus wavelength for as deposited and annealed FeS_2 thin film

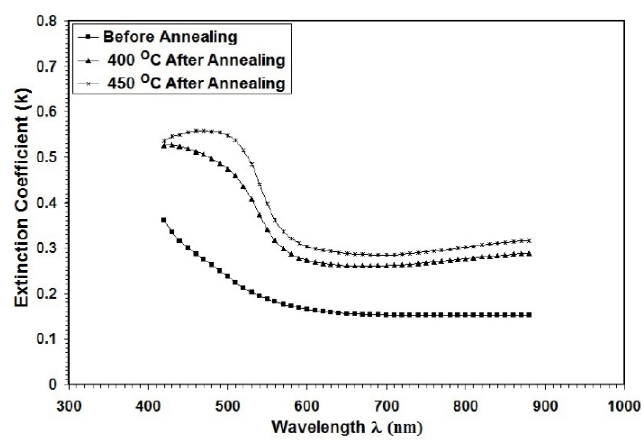

Figure 5 : Extension coefficient versus wavelength for as deposited and annealed FeS_2 thin films

Full Paper

The calculated values of extinction coefficient k versus λ for FeS_2 films are illustrated in Figure 5. It could be noticed that k values increases with increasing the wavelength and also increased as the films annealed to 400 ºC and 450ºC.

The obtained values of n and k were used to calculate both ε_1 and imaginary ε_2 parts of the dielectric constant and they were obtained using the formulas[30]:

$$\varepsilon_1 = n^2 - k^2 \quad (5)$$

$$\varepsilon_2 = 2nk \quad (6)$$

Where ε_1 determines the maximum energy that can be stored in the material, ε_2 also is called the relative loss factor and represents the absorption of electrical energy by a dielectric material that is subjected to an alternating electromagnetic field. The variation of both real ε_1 and imaginary ε_2 parts of the dielectric constant for FeS_2 films (before and after annealing) as a function of wavelength is shown in Figures 6 and 7. It can be noticed that the values of the real part are higher than those of the imaginary part. The ε_1 increase forward as the wavelength increases and display a maximum starting around 520nm which corresponds to the direct energy gap. Also the ε_2 values of the dielectric are found to be increases after annealing.

The skin depth could be calculated using the following relation[31]:

$$\chi = \lambda / 2\pi k \quad (7)$$

Where λ is the wavelength of the incident photon, k is the extinction coefficient. Figure 8 show the variation of skin depth as a function of wavelength for all films. It is clear from the figure that the skin depth increase as the wavelength increase, this behavior could be seen in all samples, but the skin depth decreases as the annealing

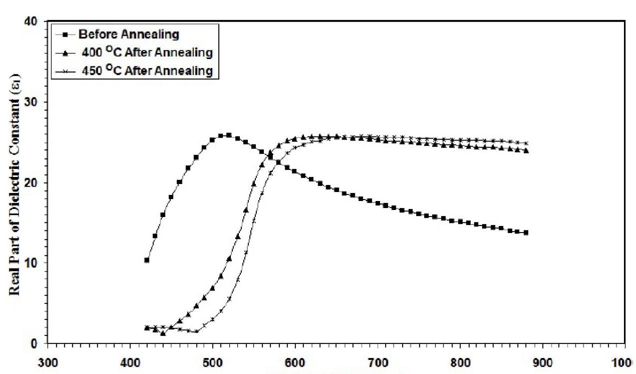

Figure 6 : Real part of the dielectric constant for as deposited and annealed FeS_2 films

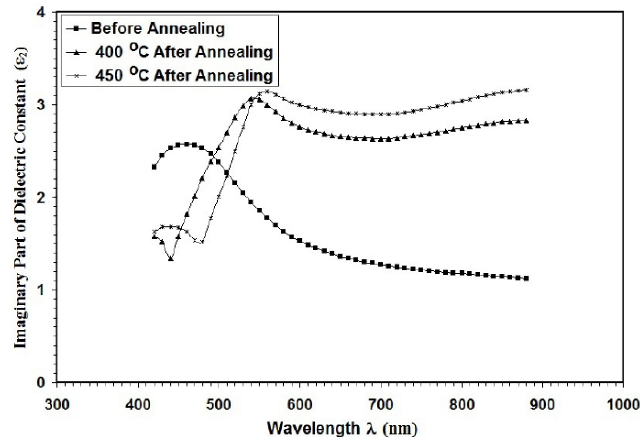

Figure 7 : Imaginary part of the dielectric constant for as deposited and annealed FeS_2 films

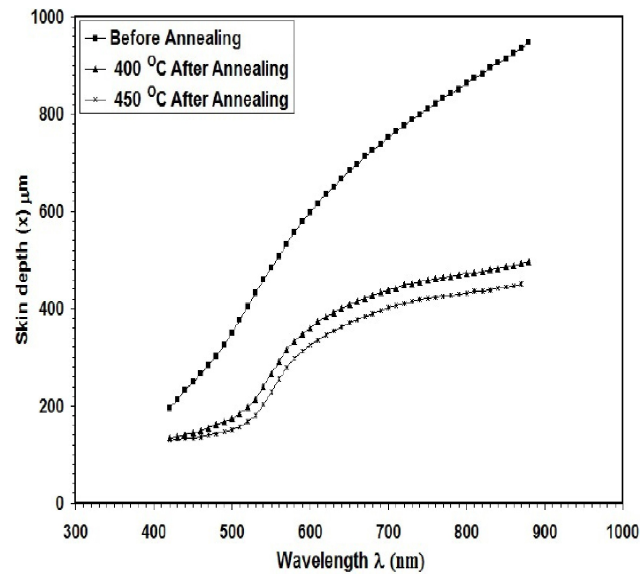

Figure 8 : Skin depth versus wavelength for as deposited and annealed FeS_2 thin films

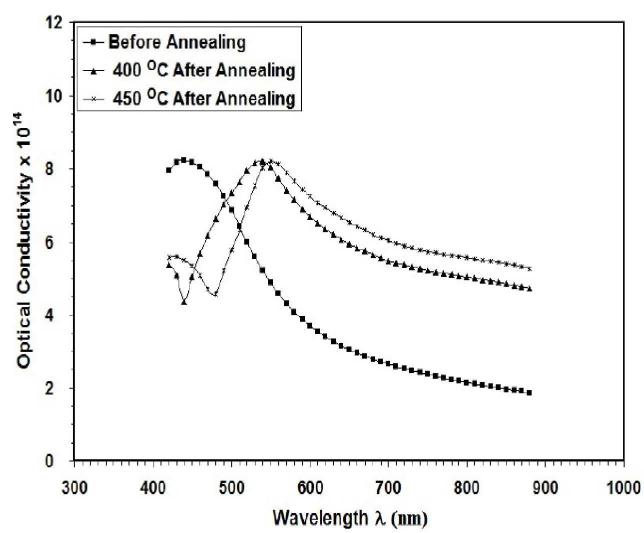

Figure 9 : Optical conductivity versus wavelength for as deposited and annealed FeS_2 films

temperature increases to 450ºC, which means that the skin depth is a transmittance related.

The optical conductivity was calculated using the relation[32]:

$$\sigma = \alpha n c / 4\pi \quad (8)$$

Where (c) is the velocity of light.

Figure 9 shows the variation of optical conductivity with the wavelength. It was observed that the optical conductivity increases with the increasing of annealing temperature. Also, It can be noticed that the optical conductivity for all films increased in the high photon energies region and decreased in the low photon energy region, this decrease is due to the low absorbance of the films in that region. This suggests that the increase in optical conductivity is due to electrons excited by photon energy. The origin of this increasing may be attributed to some changes in the structure due to the annealing and the charge ordering effect.

CONCLUSION

FeS_2 thin films have been successfully deposited onto a glass substrate by the spray pyrolysis technique. All samples were optically characterized by using UV-VIS technique and the results were systematically presented. It was found that the transmittance of the as deposited films in the visible domain reaches 45% while it decreases to 25% and 20% with increasing the annealing temperature to 400 and 450ºC respectively. Results indicate that the optical parameters are strongly dependent on annealing, as the annealing temperature increases, the absorption coefficient, extinction coefficient, real and imaginary parts of dielectric constant were calculated and they are tending to decrease with increasing annealing temperature, on the other hand the skin depth decreases with increasing annealing temperature. Further results show that the films have a high optical conductivity of about 4.06-6.20 x $10^{14}S^{-1}$. These present observations can help improve the understanding of the optical parameters of FeS_2 thin films.

REFERENCES

[1] C.de las Herasa, G.Lifante; Optical parameters of pyrite thin films, J.Appl.Phys., **82**, 5132 **(1997)**.

[2] I.J.Ferrer, D.M.Nevskaia, C.de las Heras, C.Sánchez; About the band gap nature of FeS_2 as determined from optical and photoelectrochemical measurements, Solid State Communications, **74**, 913-16 **(1990)**.

[3] K.Büker, N.Alonso Vante, H.Tributsch; Photovoltaic output limitation of n FeS_2 (pyrite) Schottky barriers: A temperature dependent characterization, J.Appl.Phys., http://dx.doi.org/10.1063/1.351925, **72**, 5721-5729 **(1992)**.

[4] P.P.Altermatt. T.Kiesewetter, K.Ellmer, H.Tributsch; Specifying targets of future research in photovoltaic devices containing pyrite (FeS_2) by numerical modeling, Solar Energy Mater.Solar Cells, **72**, 181-195 **(2002)**.

[5] A.Ennaoui, S.Fiechter, Ch.Pettenkofer, N.Alonso-Vante, K.Büker, M.Bronold, Ch.Höpfner, H.Tributsch; Iron Disulfide for Solar Energy Conversion, Solar Energy Mater.Solar Cells, **29**, 289-370 **(1993)**.

[6] J.Ferrer, D.M.Nevskaia, C.de las Heras, C.Sánchez; About the band gap nature of FeS2 as determined from optical and photoelectrochemical measurements, Solid State Commun., **74**, 913-916 **(1990)**.

[7] A.Ennaoui, S.Fiechter, H.Goslowsky, H.Tributsch; Photoactive Synthetic Polycrystalline Pyrite (FeS_2), J.Electrochem.Soc., **132**, 1579-1582 **(1985)**.

[8] J.Ferrer, C.Sanchez; Characterization of FeS_2 thin films prepared by thermal sulfidation of flash evaporated iron, J.Appl.Phys., http://dx.doi.org/10.1063/1.349377, **70**, 2641-2647 **(1991)**.

[9] S.Nakamura, A.Yamamoto; Electrodeposition of pyrite (FeS_2) thin films for photovoltaic cells, Solar Energy Mater.Solar Cells, **65**, 79-85 **(2001)**.

[10] L.Meng, Y.H.Liu, W.Huang; Synthesis of pyrite thin films obtained by thermal-sulfurating iron films at different sulfur atmosphere pressure, Mater.Sci.Eng.B., **90**, **(2002)** 84-89.

[11] N.Hamdadou, A.Khelil, J.C.Bernede; Pyrite FeS_2 films obtained by sulphuration of iron pre-deposited films, Mater.Chem.Phys., **78**, 591-601 **(2003)**.

[12] J.Oertel, K.Ellmer, W.Bohne, J.Röhrich, H.Tributsch; Growth of n-type polycrystalline pyrite (FeS_2) films by metalorganic chemical vapour deposition and their electrical characterization, J.Crystal Growth, **198-199**, 1205-1210 **(1999)**.

[13] M.Birkholz, D.Lichtenberger, C.Hopfner, S.Fiechter; Sputtering of Thin Pyrite Films, Solar Energy Mater.Sol.Cells, **27**, 243-251 **(1992)**.

[14] A.Yamamoto, M.Nakamura, A.Seki, E.L.Li, A.Hashimoto, S.Nakamura; Pyrite (FeS_2) thin films prepared by spray method using $FeSO_4$ and $(NH_4)_2Sx$, Solar Energy Mater.Solar Cells, **75**, 451-456 **(2003)**.

[15] A.S.Arico, V.Antonucci, P.L.Anntonucci, D.L.Cocke, N.Giordano; A voltammetric study of the electrodeposition chemistry in the FeS system, Electrochem.Acta, **36**, 581-590 **(1991)**.

[16] S.Nakamura, A.Yamamoto; Electrodeposition of pyrite tin films for potovoltaic cells, Sol.Energy Mater.Sol.Cells, **65**, 79-85 **(2001)**.

[17] A.Thomas, T.Cibik, C.Höpfner, K.Diesner, G.Ehlers, S.Fiechter, K.Ellmer; Formation of secondary iron-sulphur phases during the growth of polycrystalline iron pyrite (FeS_2) thin films by MOCVD, J.Mater.Sci.: Mater. in Electronics, **9**, 61-64 **(1998)**.

[18] Nafise E'jazi, Mahmoud Aghaziarati; Determination of optimum condition to produce nanocrystalline pyrite by solvothermal synthesis method, Advanced Powder Technology, **23**, 352–357 **(2012)**.

[19] G.Willeke, R.Dasbach, B.Sailer, E.Bucher; Thin pyrite (FeS_2) films prepared by magnetron sputtering, Thin Solid Films, **213**, 271-276 **(1992)**.

[20] Rachel Morrish, Rebecca Silverstein, Colin A.Wolden; Synthesis of Stoichiometric FeS_2 through Plasma-Assisted Sulfurization of Fe_2O_3 Nanorods, J.Am.Chem.Soc., **43**, 17854–17857 **(2012)**.

[21] N.Benramdane, M.Latrache, H.Tabet, M.Boukhalfa, Z.Kebbab, A.Bouzidi; Structural and optical properties of spray-pyrolysed Bi_2S_3 thin films, Mater.Sci.Eng.B., **64**, 84-87 **(1999)**.

[22] H.Tabet-Derraz, N.Benramdane, D.Nacer, A.Bouzidi, M.Medles; Investigations on $ZnxCd_{1-}xO$ thin films obtained by spray pyrolysis, Sol.Energy Mater.Sol.Cells, **73**, 249-259 **(2002)**.

[23] M.Medles, N.Benramdane, A.Bouzidi, A.Nakrela, H.Tabet-Derraz, Z.Kebbab, C.Mathieu, B.Khelifa, R.Desfeux; Optical and electrical properties of Bi_2S_3 films deposited by spray pyrolysis, Thin Solid Films, **497**, 58-64 **(2006)**.

[24] M.Birkholz, S.Fiechter, A.Hartmann, H.Tributsch; Sulfur deficiency in iron pyrite (FeS_{2-x}) and its consequences for band-structure models, Phys.Rev.B, **43(14)**, 11926-11936 **(1991)**.

[25] A.kassim, T.W.Tee, D.K.Abdullah, A.M.Sharif, H.Soon Min, G.S.Yong, S.Nagalingam; Preparation and Characteristic of iron sulphide thin films by CBD method, Indo.J.Chem., **10(1)**, 8-11 **(2010)**.

[26] L.Meng, Y.H.Liu, L.Tian; Structural, optical and electrical properties of polycrystalline pyrite (FeS_2) films obtained by thermal sulfuration of iron films, Journal of Crystal growth, http://www.paper.edu.cn, **253**, 530-538 **(2003)**.

[27] Z.S.El Mandouh, M.S.Selim; Physical properties of vanadium pentoxide sol gel films, Thin Solid Films, **371**, 259-263 **(2002)**.

[28] M.R.Islam, Podder; Optical properties of ZnO nano fiber thin films grown by spray pyrolysis of zinc acetate precursor, J.Cryst.Res.Technol., **44**, 286-292 **(2009)**.

[29] H.E.Atyia; Influence of deposition temperature on the structural and optical properties of InSbSe3 films, Optoelectron.Adv.M., **8**, 1359-1366 **(2006)**.

[30] F.Buet, J.Olivier-Fourcade, Y.Bensimon, P.Belougne; Complex Impedance Study of Chalcogenide Glasses, Solid State Communications, **77**, 29-32 **(1991)**.

[31] J.F.Eloy; 'Power Lasers', National School of Physics, Grenoble, France, John.Wiley and Sons., **59**, **(1984)**.

[32] J.I.Pankove; Optical Processes in Semiconductors, Dover Publications, Inc., New York, 91 **(1975)**.